CORONAVIRUS

Phenotype and kinetics of SARS-CoV-2–specific T cells in COVID-19 patients with acute respiratory distress syndrome

Daniela Weiskopf[1]*, Katharina S. Schmitz[2]*, Matthijs P. Raadsen[2], Alba Grifoni[1], Nisreen M. A. Okba[2], Henrik Endeman[3], Johannes P. C. van den Akker[3], Richard Molenkamp[2], Marion P. G. Koopmans[2], Eric C. M. van Gorp[2], Bart L. Haagmans[2], Rik L. de Swart[2], Alessandro Sette[1,4,5†], Rory D. de Vries[2†‡]

SARS-CoV-2 has been identified as the causative agent of a global outbreak of respiratory tract disease (COVID-19). In some patients, the infection results in moderate to severe acute respiratory distress syndrome, requiring invasive mechanical ventilation. High serum levels of IL-6 and IL-10, and an immune hyperresponsiveness referred to as a "cytokine storm," have been associated with poor clinical outcome. Despite the large numbers of COVID-19 cases and deaths, information on the phenotype and kinetics of SARS-CoV-2–specific T cells is limited. Here, we studied 10 patients with COVID-19 who required admission to an intensive care unit and detected SARS-CoV-2–specific $CD4^+$ and $CD8^+$ T cells in 10 of 10 and 8 of 10 patients, respectively. We also detected low levels of SARS-CoV-2–reactive T cells in 2 of 10 healthy controls not previously exposed to SARS-CoV-2, which is indicative of cross-reactivity due to past infection with "common cold" coronaviruses. The strongest T cell responses were directed to the spike (S) surface glycoprotein, and SARS-CoV-2–specific T cells predominantly produced effector and T helper 1 (T_H1) cytokines, although T_H2 and T_H17 cytokines were also detected. Furthermore, we studied T cell kinetics and showed that SARS-CoV-2–specific T cells are present relatively early and increase over time. Collectively, these data shed light on the potential variations in T cell responses as a function of disease severity, an issue that is key to understanding the potential role of immunopathology in the disease, and also inform vaccine design and evaluation.

INTRODUCTION

A novel coronavirus named SARS-CoV-2 has been identified as the causative agent of a global outbreak of respiratory tract disease, referred to as coronavirus disease 2019 (COVID-19) (*1*, *2*). COVID-19 is characterized by fever, cough, dyspnea, and myalgia (*2*), but, in some patients, the infection results in moderate to severe acute respiratory distress syndrome (ARDS), requiring invasive mechanical ventilation for a period of several weeks. Patients with COVID-19 may present with lymphopenia (*2*, *3*), but the disease has also been associated with immune hyperresponsiveness referred to as a "cytokine storm" (*4*). A transient increase in coexpression of CD38 and human leukocyte antigen (HLA)–DR by T cells, a phenotype of $CD8^+$ T cell activation in response to viral infection, was observed concomitantly (*5*). This increase in both $CD4^+$ and $CD8^+$ $CD38^+$ HLA-DR^+ T cells preceded resolution of clinical symptoms in a nonsevere, recovered, COVID-19 patient (*6*).

Despite the large numbers of cases and deaths, there is limited information on the presence and phenotype of SARS-CoV-2–specific T cells, especially in patients with ARDS. Spike surface glycoprotein (S)–, membrane (M)–, and nucleoprotein (NP)–specific T cells were detected in peripheral blood mononuclear cells (PBMCs) from convalescent COVID-19 patients (*7*). More recently, Grifoni *et al.* (*8*) reported the presence of SARS-CoV-2–specific T cells in convalescent samples from predominantly mild COVID-19 patients. They showed strong reactivity to the viral S and M proteins and also strong $CD4^+$ T cell responses to N. In addition, eight other open reading frames were targeted by both $CD4^+$ and $CD8^+$ T cells. Virus-specific T cells have also been detected after exposure to the related SARS-CoV and MERS-CoV, although few studies have characterized cellular responses in human patients. For SARS-CoV–specific $CD4^+$ T cells, it was reported that the S glycoprotein is responsible for nearly two-thirds of T cell reactivity, with N and M also accounting for limited reactivity (*9*). For MERS-CoV–specific $CD4^+$ T cells, responses targeting S, N, and a pool of M and E peptides have been reported (*10*).

Here, we stimulated PBMCs from 10 COVID-19 patients with ARDS, collected up to 3 weeks after admission to the intensive care unit (ICU), with MegaPools (MPs) of overlapping or prediction-based peptides covering the SARS-CoV-2 proteome (*11*). We detected SARS-CoV-2–specific $CD4^+$ and $CD8^+$ T cells in 10 of 10 and 8 of 10 patients with COVID-19, respectively. Peptide stimulation of healthy control (HC) age-matched PBMC samples collected before the outbreak in most cases resulted in undetectable responses, although some potential cross-reactivity due to infection with "common cold" coronaviruses was observed. SARS-CoV-2–specific T cells predominantly produced effector and T helper 1 (T_H1) cytokines, although T_H2 and T_H17 cytokines were also detected.

RESULTS

Patient characteristics

We included 10 COVID-19 patients with moderate to severe ARDS in this study and compared these with 10 age-matched HCs. All patients were included in the study shortly after ICU admission; the

[1]Center for Infectious Disease, La Jolla Institute for Immunology, La Jolla, CA 92037, USA. [2]Department of Viroscience, Erasmus MC, Rotterdam, the Netherlands. [3]Department of Intensive Care, Erasmus MC, Rotterdam, the Netherlands. [4]Department of Pathology, University of California, San Diego, CA 92037, USA. [5]Department of Medicine, University of California, San Diego, CA 92037, USA.
*These authors contributed equally to this work as first authors.
†These authors contributed equally to this work as last authors.
‡Corresponding author. Email: r.d.devries@erasmusmc.nl

duration of self-reported illness varied between 5 and 14 days before inclusion (Fig. 1A). Patients were between 49 and 72 years old (average 58.9 ± 7.2 years) and of mixed gender (four females and six males). HC were between 30 and 66 years old (average 43 ± 13.6 years, not statistically different from the patient group) and of mixed gender (four females, four males, and no data available for two donors). All patients tested SARS-CoV-2 positive by reverse transcription polymerase chain reaction (RT-PCR) and were ventilated during their stay at the ICU. At the time of writing, five patients were transferred out of the ICU (cases 1, 2, 4, 6, and 7), three patients were still in follow-up (cases 5, 9, and 10), one patient was discharged (case 8), and one patient was deceased (case 3). Case 4 died 4 days after transfer out of the ICU. Patients were treated with lung protective ventilation using the higher positive end-expiratory pressure (PEEP)/lower FiO_2 table of the ARDSnet and restrictive volume resuscitation. They received antibiotics as a part of a treatment regimen aimed at selective decontamination of the digestive tract. Furthermore, all patients received chloroquine, lopinavir-ritonavir, and/or corticosteroids for a brief period of time around admission to the ICU (Fig. 1A).

COVID-19 ARDS patients present with lymphopenia

Phenotyping analysis of PBMCs collected 14 days after inclusion via flow cytometry indicated that patients with COVID-19 presented with low percentages of $CD3^+$ T cells in peripheral blood, corresponding to the previously reported lymphopenia (12.1 ± 8.7% in COVID-19 versus 44.3 ± 7.1% in HCs, $P < 0.0001$; Fig. 1B) (*2*, *3*). CD4:CD8 ratios were increased in patients with COVID-19 when compared with HCs (5.5 ± 3.0 in COVID-19 versus 2.3 ± 0.9 in HCs, $P = 0.0115$; Fig. 1C).

SARS-CoV-2 peptides and predicted epitopes

PBMCs from COVID-19 ARDS patients were stimulated with four different peptide MPs: MP_S, MP_CD4_R, and two MP_CD8 pools. MP_S contained 221 overlapping peptides (15-mers overlapping by 10 amino acids) covering the entire S glycoprotein and can stimulate both $CD4^+$ and $CD8^+$ T cells. MP_CD4_R (R = remainder) contained 246 HLA class II predicted epitopes covering all viral proteins except S, specifically designed to activate $CD4^+$ T cells. The two MP_CD8 pools combined contained 628 HLA class I predicted epitopes covering all SARS-CoV-2 proteins, specifically designed to activate $CD8^+$ T cells (*11*). Results obtained with MP_CD8_A and MP_CD8_B have been concatenated and shown as a combined stimulation named MP_CD8, but results obtained with separate stimuli are also shown. In addition to stimulation of PBMCs from COVID-19 ARDS patients, PBMCs from 10 HCs were tested in parallel. PBMCs from HCs were obtained before 2020 and could therefore not contain SARS-CoV-2–specific T cells. However, they potentially contain cross-reactive T cells induced by circulating seasonal common cold coronaviruses (*12*).

Stimulation of PBMCs collected 14 days after inclusion with the different peptide pools led to consistent detection of $CD4^+$ and/or $CD8^+$ SARS-CoV-2–specific T cells in COVID-19 ARDS patients (Figs. 2 and 3). Specific activation of $CD4^+$ and $CD8^+$ T cells was measured via cell surface expression of CD69 and CD137; phenotyping of memory subsets was based on surface expression of CD45RA and CCR7 (fig. S1).

Characterization of SARS-CoV-2–specific $CD4^+$ T cell responses

Stimulation of PBMCs with MP_S and MP_CD4_R led to consistent activation of SARS-CoV-2–specific $CD4^+$ T cells (Fig. 2) in PBMCs

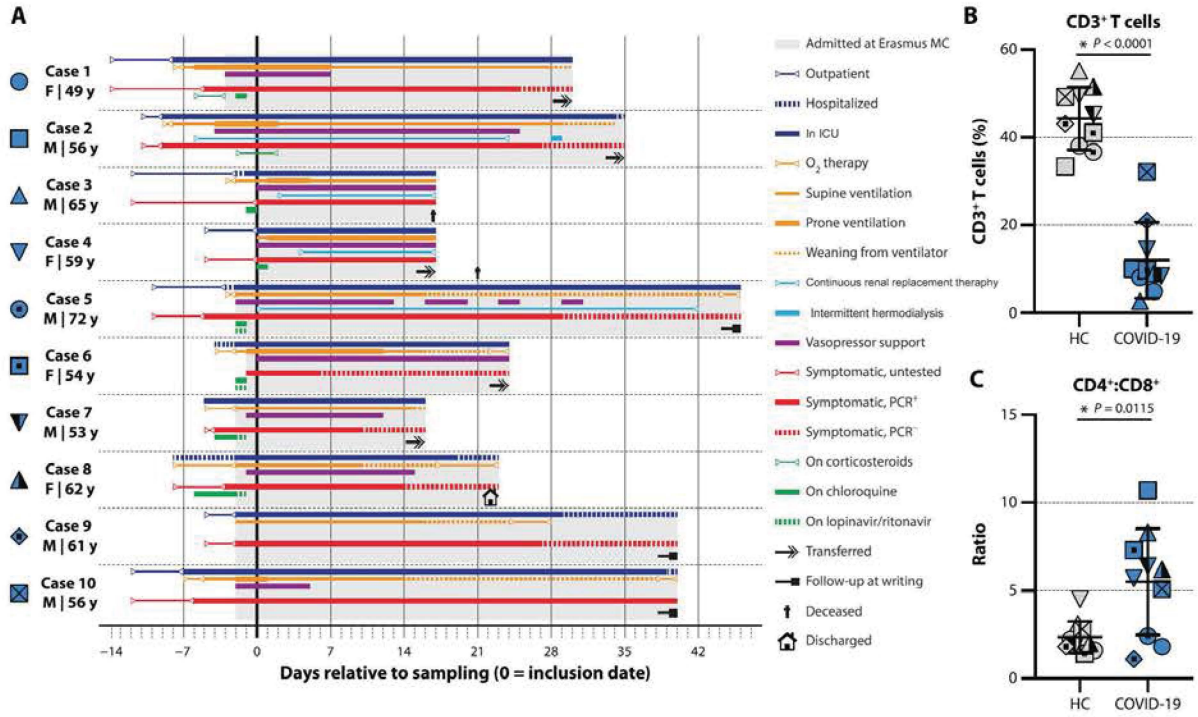

Fig. 1. Clinical overview of moderate to severe COVID-19 ARDS patients. (**A**) Onset of symptoms, hospitalization status, treatment, and follow-up of $n = 10$ COVID-19 ARDS patients included in this study. PBMC samples were obtained weekly after admission to the study. Symbols shown next to the cases match throughout all figures. (**B**) Percentages of $CD3^+$ T cells within the total LIVE gate measured by flow cytometry performed on PBMC collected 14 days after inclusion. (**C**) CD4:CD8 ratios measured by flow cytometry performed on PBMC collected 14 days after inclusion. (B) and (C) show individual values for $n = 10$ patients versus $n = 10$ HC, as well as the mean ± SD. Asterisks denote significant differences.

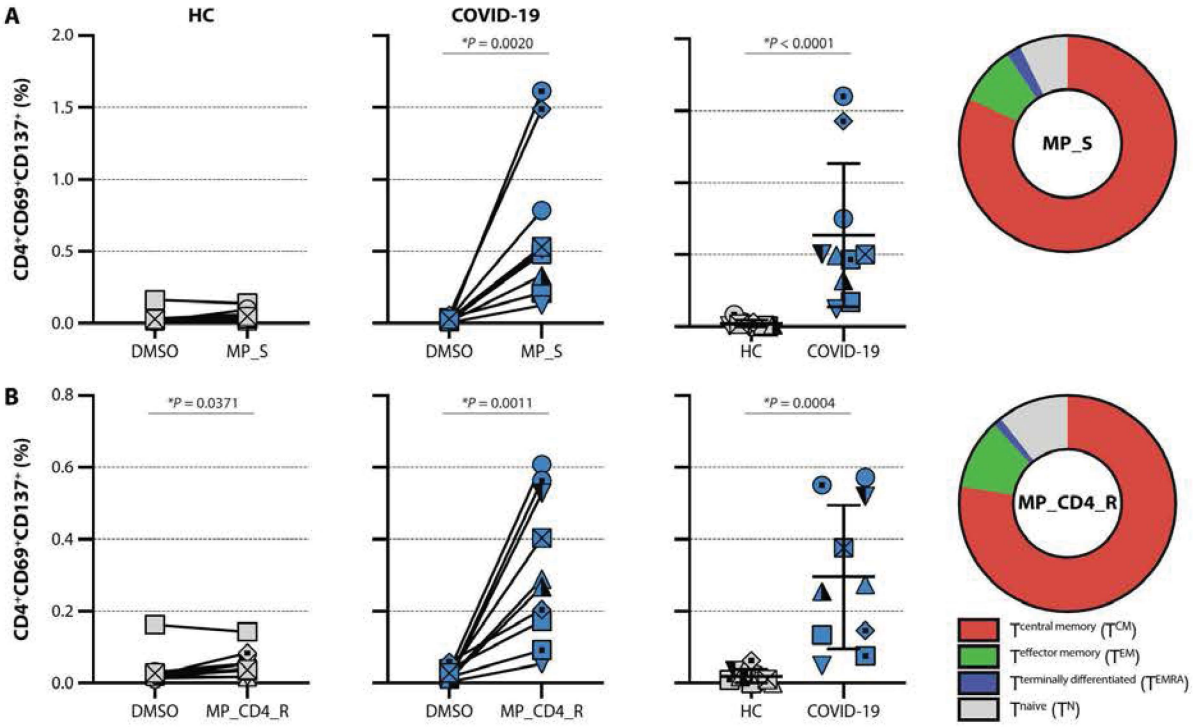

Fig. 2. SARS-CoV-2–specific CD4$^+$ T cell responses in COVID-19 ARDS patients. (**A** and **B**) Antigen-specific activation of CD4$^+$ T cells after stimulation for 20 hours with MP_S (A) and MP_CD4_R (B) measured via cell surface expression of CD69 and CD137 (gating in fig. S1). Two left panels show activation percentages (within CD3$^+$CD4$^+$) obtained with the vehicle control (DMSO) and specific stimulation (MP) for HC and patients with COVID-19. The third panel shows the specific activation percentages corrected by subtracting the background present in the DMSO stimulation to allow comparison of both groups. The fourth panel shows the memory phenotype of the CD69$^+$CD137$^+$ responder cells in a donut diagram. Panels show individual values for $n = 10$ patients versus $n = 10$ HC, as well as the mean ± SD. Asterisks denote significant differences. Symbol shapes of patients with COVID-19 are identical between panels and refer back to Fig. 1.

obtained from COVID-19 ARDS patients. Substantial responses were detected when activation percentages after stimulation with MP_S and MP_CD4_R were compared with the vehicle control [dimethyl sulfoxide (DMSO)]. To allow comparison between HCs and COVID-19 ARDS patients, we corrected the MP-specific activation percentages by subtracting the value obtained in the DMSO stimulation. Significant T cell responses were observed in COVID-19 ARDS patients when compared with HCs (0.64% in COVID-19 versus 0.02% in HCs, $P < 0.0001$ for MP_S and 0.29% in COVID-19 versus 0.02% in HCs, $P = 0.0004$ for MP_CD4_R; Fig. 2, A and B, respectively). The stimulation index (SI) was calculated by dividing the MP-specific responses by the DMSO responses, and donors with a SI > 3 were regarded responders (Fig. 4A). According to this definition, all COVID-19 ARDS patients responded to the MP_S and MP_CD4_R pools, whereas 1 of 10 and 2 of 10 of the HC responded, respectively (Fig. 7). Overall, the MP_S peptide pool induced stronger responses than the MP_CD4_R peptide pool, indicating that the S glycoprotein is a strong inducer of CD4$^+$ T cell responses. Phenotyping of CD4$^+$CD69$^+$CD137$^+$-activated T cells identified the majority of these SARS-CoV-2–specific T cells as central memory T cells, based on CD45RA and CCR7 expression (T_{CM}). T_{CM} express homing receptors required for extravasation and migration to secondary lymphoid tissues but also have high proliferative capacity with low dependence on costimulation (*13*, *14*).

Characterization of SARS-CoV-2–specific CD8$^+$ T cell responses

SARS-CoV-2–specific CD8$^+$ T cells were activated by both the MP_S and MP_CD8 peptide pools when compared with vehicle control (Fig. 3, A and B). Mainly, the peptides pooled in MP_CD8_A were responsible for this activation (Fig. 3, C and D). Furthermore, significant responses were detected when activation percentages after stimulation with MP_S and MP_CD8 were compared between HC and COVID-19 ARDS patients after DMSO correction (0.90% in COVID-19 versus 0.03% in HCs, $P = 0.0003$ for MP_S and 0.57% in COVID-19 versus 0.03% in HCs, $P < 0.0001$ for MP_CD8; Fig. 3, A and B). In addition to inducing specific CD4$^+$ T cells, the S glycoprotein also induced CD8$^+$ T cell responses. Calculation of the SI identified 8 of 10 and 4 of 9 (not enough cells were obtained for MP_CD8 stimulation for one donor) of the COVID-19 ARDS patients as responders to MP_S and MP_CD8, respectively, whereas 1 of 10 of the HCs responded to the MP_S stimulation (Figs. 4, B and C, and 7). Phenotyping of CD8$^+$CD69$^+$CD137$^+$-activated T cells showed that these had a mixed phenotype. The majority of virus-specific CD8$^+$ T cells was identified as CCR7$^-$ effector memory (T_{EM}) or terminally differentiated effector (T_{EMRA}) (*13*). Both these CD8$^+$ effector subsets are potent producers of interferon-γ (IFN-γ), contain preformed perforin granules for immediate antigen-specific cytotoxicity, and home efficiently to peripheral lymphoid tissues (*14*, *15*).

Cytokine profiles after antigen-specific stimulation

Because production of proinflammatory cytokines can be predictive of clinical outcome for other viral diseases (*16*), we measured antigen-specific production of 13 cytokines in cell culture supernatants from PBMCs after stimulation. The same samples as shown in Figs. 1 to 4 were included in this analysis, using samples obtained 14 days after

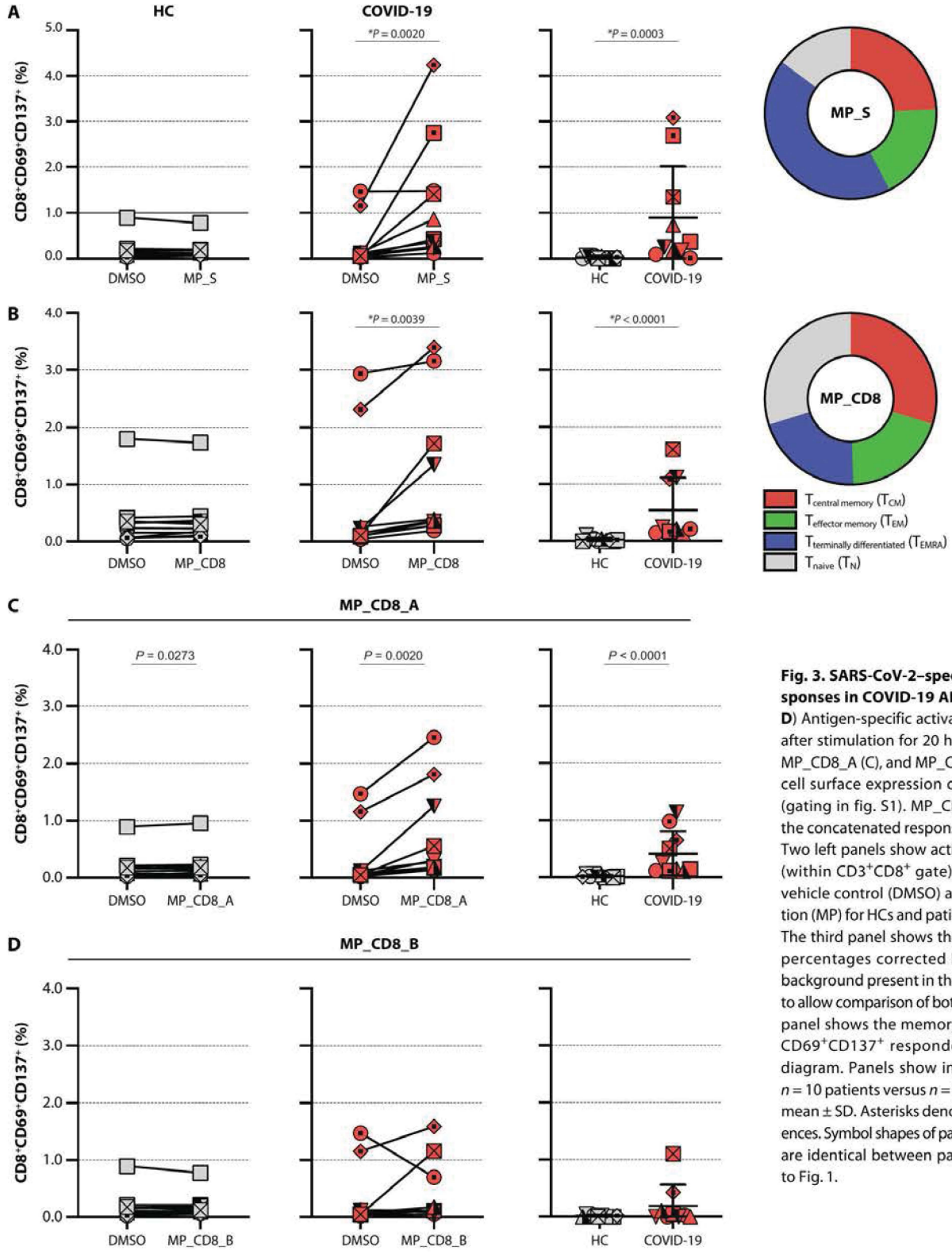

Fig. 3. SARS-CoV-2–specific CD8$^+$ T cell responses in COVID-19 ARDS patients. (**A** to **D**) Antigen-specific activation of CD8$^+$ T cells after stimulation for 20 hours with MP_S (A), MP_CD8_A (C), and MP_CD8_B, measured via cell surface expression of CD69 and CD137 (gating in fig. S1). MP_CD8 panels (B) show the concatenated responses from (C) and (D). Two left panels show activation percentages (within CD3$^+$CD8$^+$ gate) obtained with the vehicle control (DMSO) and specific stimulation (MP) for HCs and patients with COVID-19. The third panel shows the specific activation percentages corrected by subtracting the background present in the DMSO stimulation to allow comparison of both groups. The fourth panel shows the memory phenotype of the CD69$^+$CD137$^+$ responder cells in a donut diagram. Panels show individual values for $n = 10$ patients versus $n = 10$ HC, as well as the mean ± SD. Asterisks denote significant differences. Symbol shapes of patients with COVID-19 are identical between panels and refer back to Fig. 1.

ICU admission. PBMCs were stimulated with the respective peptide pools, cytokine production after MP_S stimulation is shown in Fig. 5 and fig. S2 as representative data. When compared with the vehicle control stimulation, PBMCs obtained from COVID-19 ARDS patients specifically produced IFN-γ, tumor necrosis factor–α (TNF-α), interleukin-2 (IL-2), IL-5, IL-13, IL-10, IL-9, IL-17A, IL-17F, and IL-22 after MP_S stimulation (Fig. 5 and fig. S2).

When comparing COVID-19 ARDS patients with HC, stimulation of PBMCs by the overlapping S peptide pool led to a strong significant production of the T_H1 or effector cytokines IFN-γ, TNF-α,

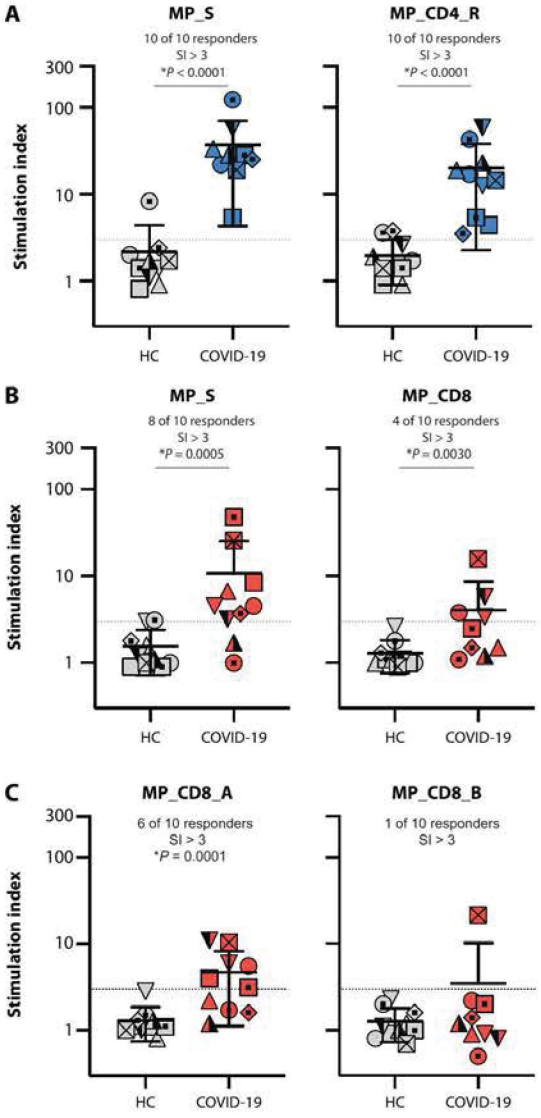

Fig. 4. SI identifies specific responders. Antigen-specific activation of $CD4^+$ (**A**) and $CD8^+$ T cells (**B** and **C**) in patients with COVID-19 after stimulation for 20 hours with peptide MPs is shown as SI. SI is derived by dividing the percentage obtained with specific stimulation (MP) by the percentage obtained with the vehicle control (DMSO). Values for respective stimulations are shown in Fig. 2 ($CD4^+$, color coded in blue) and Fig. 3 ($CD8^+$, color coded in red). Donors with a SI > 3 (dotted lines) are regarded as responders to MP stimulation. Panels show individual values for $n = 10$ patients versus $n = 10$ HC, as well as the mean ± SD. Asterisks denote significant differences. Symbol shapes of patients with COVID-19 are identical between panels and refer back to Fig. 1.

and IL-2 in COVID-19 ARDS patients. More characteristic T_H2 cytokines (IL-5, IL-13, IL-9, and IL-10) were also consistently detected, albeit at low levels. IL-4 and IL-21 could not be detected at all. IL-6 levels were not different between patients with COVID-19 and HCs. However, these results were difficult to interpret because mock stimulation already resulted in high IL-6 expression. Antigen-specific production of cytokines related to a T_H17 response was also consistently detected; PBMCs from COVID-19 ARDS patients produced significantly more IL-17A, IL-17F, and IL-22 than HCs.

In general, stimulation of PBMCs from COVID-19 ARDS patients with MPs led to a dominant production T_H1 or effector cytokines (IFN-γ, TNF-α, and IL-2), but T_H2 (IL-5, IL-13, IL-9, and IL-10) and T_H17 (IL-17A, IL-17F, and IL-22) cytokines could also be detected. Although not enough COVID-19 ARDS patients were included in this study to correlate specific T cell responses to clinical outcome, we did observe differences in cytokine production profiles on a case-per-case basis (fig. S2D). Plotting the respective cytokine quantities as a percentage of total cytokine production showed that IL-6 (cases 3, 5, and 9), TNF-α (cases 1, 3, and 9), IL-2 (case 8), or IFN-γ (cases 2, 4, 6, 7, and 10) dominated the response.

Longitudinal detection of SARS-CoV-2–specific T cell responses

Last, we studied the kinetics of development of virus-specific humoral and cellular immune responses in COVID-19 ARDS patients included in this study. Real-time RT-PCR detection of SARS-CoV-2 genomes in respiratory tract samples showed a decreasing trend over time [Fig. 6A; analysis of variance (ANOVA) repeated measures, $P < 0.001$], whereas virus-specific serum immunoglobulin G (IgG) antibody levels, measured by receptor binding domain (RBD) enzyme-linked immunosorbent assay (ELISA), showed a significant increase (Fig. 6B; ANOVA repeated measures, $P < 0.001$). Concomitantly, SARS-CoV-2–specific $CD4^+$ and $CD8^+$ T cells were detected in all patients at multiple time points. For $CD4^+$ T cell responses, the frequencies of virus-specific responder cells increased significantly over time (Fig. 6C; ANOVA repeated measures, $P < 0.001$) for $CD8^+$ T cells this increase was not as apparent (Fig. 6D; ANOVA repeated measures, $P = 0.1001$). We found evidence for a direct negative correlation between viral loads and IgG ELISA ($r = 0.6630$, $P < 0.0001$) and viral loads and $CD4^+$ T cells ($r = 0.5675$, $P = 0.0007$) and a positive correlation between the appearance of IgG antibodies and virus-specific T cells ($r = 0.6360$, $P = 0.0002$) (fig. S3).

DISCUSSION

Collectively, these data provide information on the phenotype, breadth, and kinetics of virus-specific cellular immune responses in COVID-19 ARDS patients. We provide evidence that SARS-CoV-2–specific $CD4^+$ and $CD8^+$ T cells appear in blood of patients with ARDS in the first 2 weeks after the onset of symptoms. It is important to mention that this study focused on PBMC samples, but tissue-resident T cells undoubtedly play an important role in this early response. SARS-CoV-2–specific $CD4^+$ T cells in blood typically had a central memory phenotype, whereas $CD8^+$ T cells had a more effector phenotype. Peng *et al.* (*17*) also identified HLA-B*40:01–restricted T cells with mainly a central and effector memory phenotype. Consistent production in response to viral antigen of IFN-γ, TNF-α, IL-2, IL-5, IL-13, IL-9, IL-10, IL-17A, IL-17F, and IL-22 was observed, with a dominant production of the effector and T_H1 cytokines. Because of limitations in the number of PBMCs that could be obtained from severe COVID-19 ARDS patients in an ICU setting, we could not resolve which cells were responsible for production of which cytokine by intracellular cytokine staining.

Elevated levels of IL-6 in patient plasma have been correlated to respiratory failure in patients with COVID-19 (*18*). Although we could not detect increased specific production of IL-6 in PBMCs stimulated with peptide pools due to high background production in controls, we detected a dominant IL-6 and TNF-α response in cell culture supernatants from the patient deceased because of respiratory

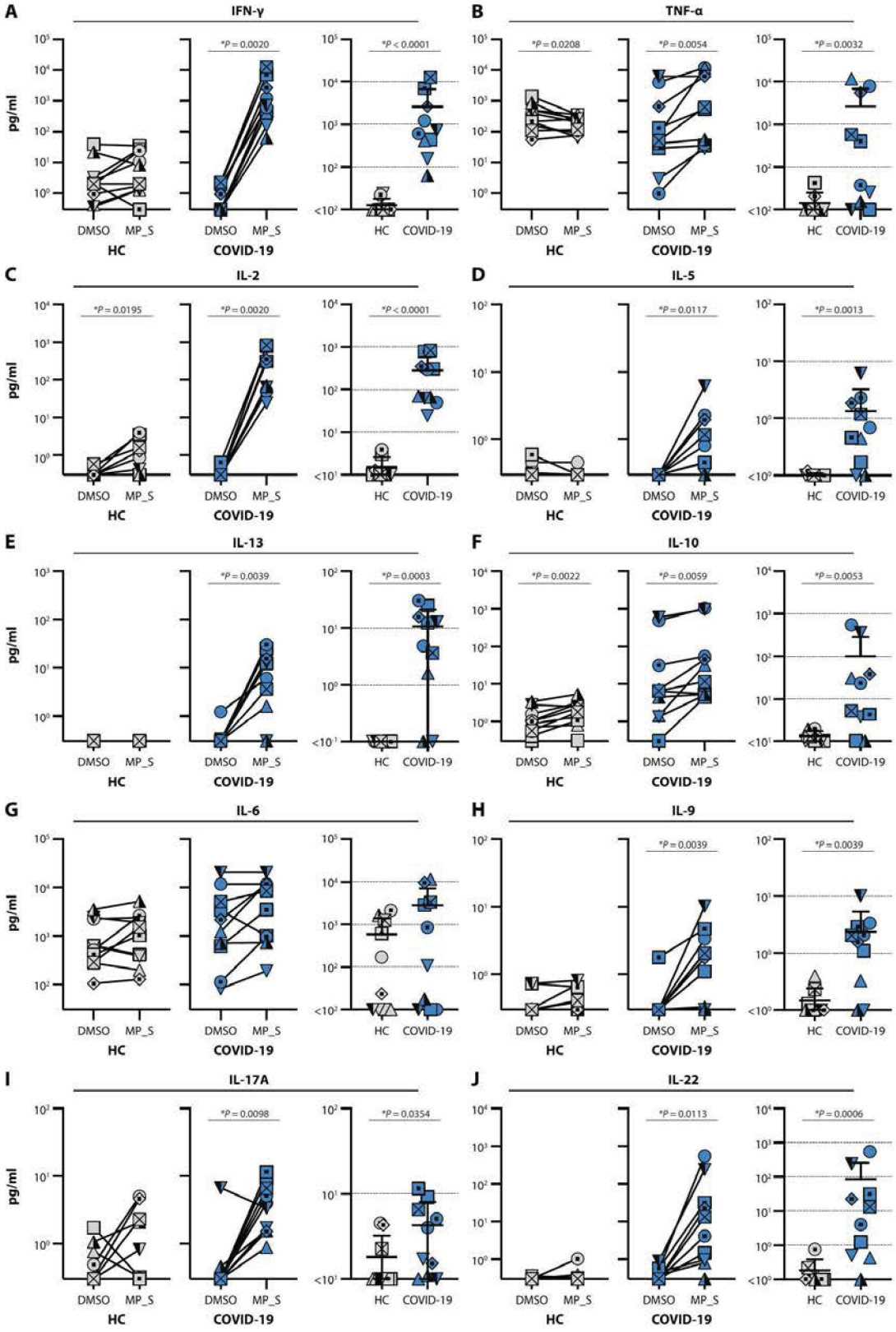

Fig. 5. SARS-CoV-2–specific cytokine production in COVID-19 ARDS patients. (**A** to **J**) Antigen-specific production of cytokines measured in cell culture supernatants from PBMC obtained 14 days after ICU admission stimulated (20 hours) with MP_S. Two left panels show quantities obtained with the vehicle control (DMSO) and specific stimulation (MP) for HC and patients with COVID-19. The third panel shows the quantity corrected by subtracting the background present in the DMSO stimulation to allow comparison of both groups. Panels show individual values for $n = 10$ patients versus $n = 10$ HC, as well as the geometric mean. Asterisks denote significant differences. Additional cytokines (IL-4, IL-17F, and IL-21) are shown in fig. S2. Symbol shapes of patients with COVID-19 are identical between panels and refer back to Fig. 1.

failure (case 3; fig. S2D). To determine the role of T cells in COVID-19, it is crucial that the cell types responsible for the production of IL-6 and the concomitant cytokine storm are identified in large comparative cohort studies.

We included PBMC obtained from 10 buffy coats obtained before the SARS-CoV-2 pandemic as negative HCs. These HCs were similar to the studied COVID-19 ARDS patients regarding age and gender. In some instances, reactive T cells were detected in HC after MP stimulation, both on basis of T cell activation and cytokine production (Figs. 4, 6, and 7). Because PBMCs from these HCs could not contain SARS-CoV-2–specific T cells, we hypothesize that these responses were cross-reactive and had been induced by circulating seasonal common cold coronaviruses. If we consider samples with a SI > 3 as responders, we identified 2 of 10 HCs (20%) to have these cross-reactive T cells. Our study reports responses in unexposed individuals in The Netherlands. This fits well with the report of Grifoni *et al.* from the United States (*8*), Braun *et al.* from Germany (*19*), Le Bert *et al.* from Singapore (*20*), and Meckiff *et al.* from the United Kingdom (*21*), who all report significant rates of reactivity from unexposed individual. Peng *et al.* (*17*) did not see significant responses potentially reflecting geographical and temporal variations or the importance of experimental conditions. It is

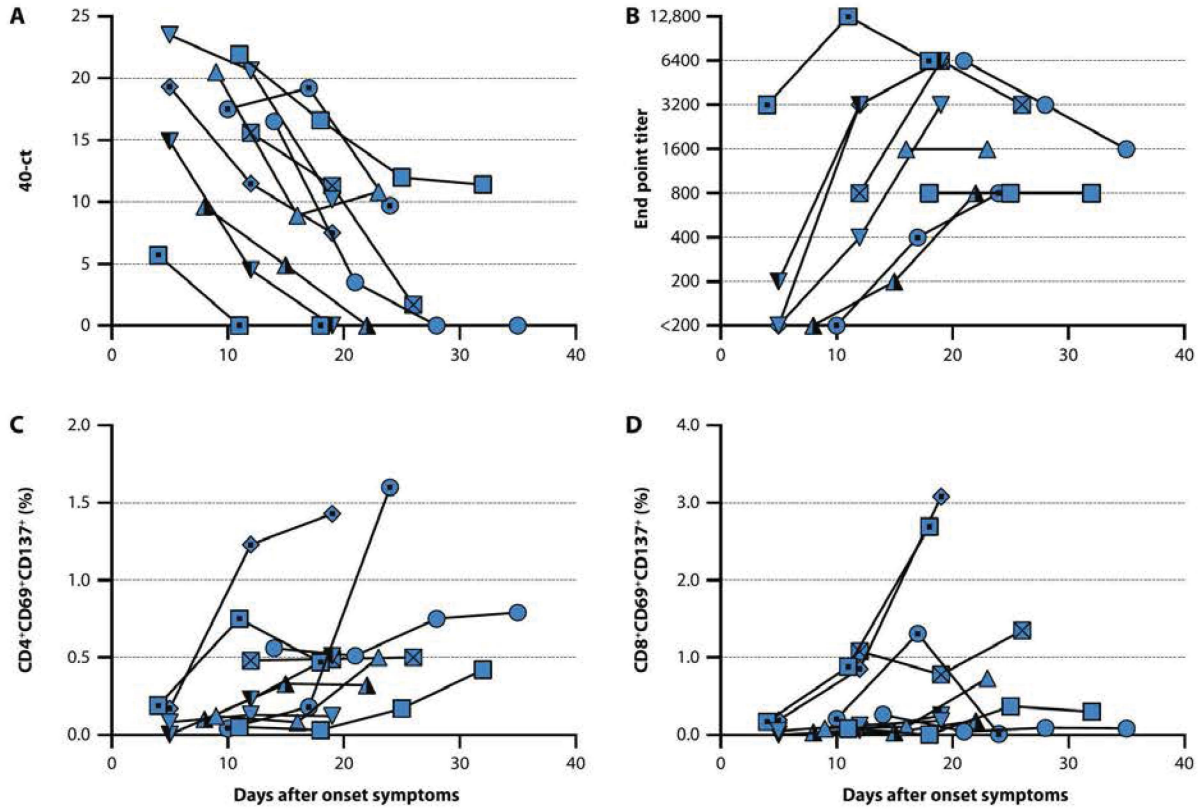

Fig. 6. SARS-CoV-2 replication and humoral and cellular immune response kinetics in COVID-19 ARDS patients. (**A** to **D**) Sequential measurements of SARS-CoV-2 genomes detected in upper respiratory tract samples by real-time RT-PCR (40-ct, A), SARS-CoV-2–specific serum RBD IgG antibody levels detected by ELISA (Endpoint titer, B), and percentage SARS-CoV-2–specific $CD4^+$ and $CD8^+$ T cells after MP_S stimulation of PBMC (C and D) plotted against days after the onset of symptoms. Genome levels showed a significant decrease over time, and antibody levels and specific $CD4^+$ T cell frequencies significantly increased ($P < 0.001$, ANOVA repeated measures). A specific increase or decrease of specific $CD8^+$ T cells over time was not detected ($P = 0.1001$, ANOVA repeated measures). Symbol shapes of patients with COVID-19 are identical between panels and refer back to Fig. 1.

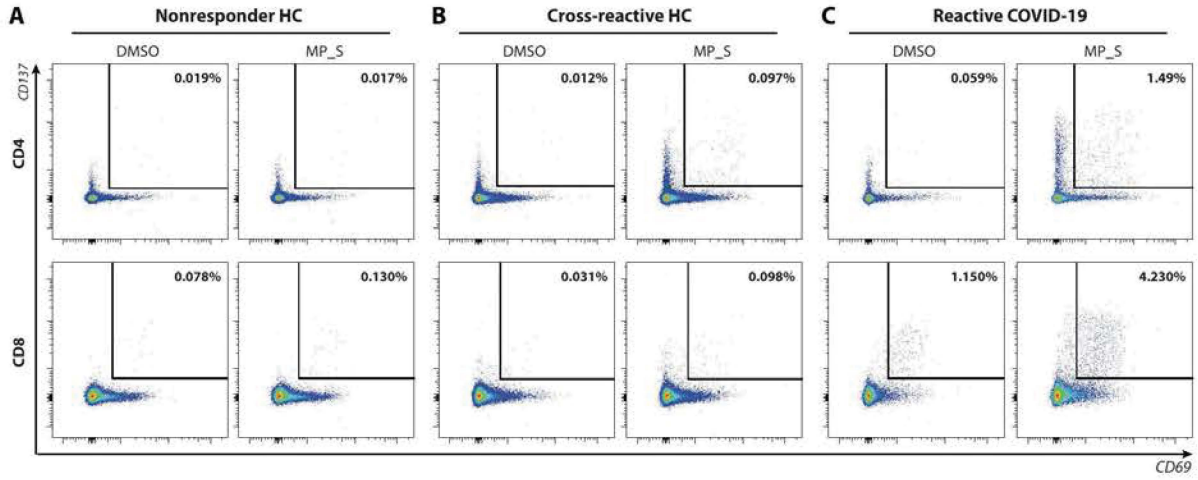

Fig. 7. Expression of activation markers in representative samples. (**A** to **C**) Representative activation plots showing CD69 and CD137 up-regulation from a nonresponder HC (A), cross-reactive HC (B), and reactive COVID-19 sample (C). Each panel shows activation after stimulation with DMSO (negative control) or MP_S. Top row shows $CD4^+$ T cell responses, and bottom row shows $CD8^+$ T cell responses. Percentages indicate activated $CD69^+CD137^+$ cells as a fraction of either $CD4^+$ or $CD8^+$ T cells. These percentages were used in the generation of Figs. 2 and 3.

possible that HLA genotypes influence these responses, as well as the SARS-CoV-2 responses that were detected in patients with ARDS. This is a topic that merits further investigation. The role of preexisting SARS-CoV-2–reactive T cells as a correlate of protection or pathology is unclear and needs to be addressed in prospective studies.

Novel SARS-CoV-2 vaccines are currently in development and mainly focus on the surface glycoprotein S as an antigen for efficient

induction of virus-specific neutralizing antibodies. We now show that S can also be a potent immunogen for inducing virus-specific $CD4^+$ and $CD8^+$ T cells. This is in good concordance with publications on related coronaviruses SARS-CoV and MERS-CoV (*9*, *10*) and also with recent reports detecting SARS-CoV-2–specific T cell responses (*7*, *8*, *17*, *19*, *22*, *23*). Our study adds to that body of literature, as we specifically studied a well-defined ARDS patient cohort and studied samples longitudinally while correlating these to viral loads, humoral responses, memory phenotypes, and cytokine response profiles.

Here, we specifically studied T cell responses in patients with ARDS admitted to the ICU. By definition, these are all patients with severe COVID-19; therefore, we cannot draw any conclusions on how the T cell responses relate to disease severity. Whether the presence and certain phenotypes of T cells are correlated to a "good" or "bad" prognosis remains to be determined. Collectively, these data shed light on the potential variations in T cell responses as function of disease severity, an issue that is key to understanding the potential role of immunopathology in the disease, as well as to inform vaccine design and evaluation.

MATERIALS AND METHODS

Study design

Here, we set out to detect and characterize SARS-CoV-2–specific $CD4^+$ and $CD8^+$ T cell responses in longitudinal PBMC samples obtained from COVID-19 ARDS patients. The patient cohort was well characterized, including 10 patients, and defined by a positive RT-PCR on a sample from the respiratory tract. From each patient, samples at multiple time points (days 0, 7, 14, and later if available) were tested. These patients were directly compared with 10 HCs.

This study relied on the use of predesigned peptide MP containing overlapping peptides or predicted epitopes for stimulation of PBMCs. T cell activation and phenotype were determined by flow cytometry, whereas cytokine production was determined by a beads-based multiplex assay. Each stimulation assay consisted of eight conditions: stimulation with four different MPs, a negative DMSO control, a negative medium control, a positive phytohemagglutinin (PHA) control, and a cytomegalovirus (CMV) control. A sample nonresponsive to PHA stimulation would have been excluded from analysis (0 occurrences); all other data were included. Because of the limited nature of the material (PBMCs from patients with ARDS), activation after stimulation was measured in single determinations. All raw data obtained are provided in tabular format in table S1.

Ethical statement

Patients admitted into the ICU with ARDS resulting from SARS-CoV-2 infection at Erasmus MC, Rotterdam, The Netherlands were included in a biorepository study aimed at ARDS and sepsis in the ICU. The first EDTA blood samples for PBMC isolation were obtained no more than 2 days after admission into the Erasmus MC ICU. Samples were collected weekly until a final sample at 28 days after study inclusion or for as long as the patient was in the ICU. Patient care and research were conducted in compliance within guidelines of the Erasmus MC and the Declaration of Helsinki. Because of the clinical state of most patients with ARDS (i.e., intubated and comatose), deferred proxy consent was obtained instead of direct written informed consent from the patients themselves. Retrospective written informed consent was obtained from patients after recovery. The study protocol was approved by the medical ethical committee of Erasmus MC, Rotterdam, The Netherlands (MEC-2017-417 and MEC-2020-0222). HC human buffy coats were requested as a comparator group at the Sanquin Blood Bank (Rotterdam, The Netherlands); written informed consent for research use was obtained. HCs were slightly younger than the included patients with COVID-19; however, this was a nonsignificant difference and we therefore consider the HC and patients with COVID-19 age matched.

Diagnosis

Real-time RT-PCR on the E-gene was performed as described previously (*24*) on RNA isolated from sputa, nasopharyngeal, or oropharyngeal swabs by MagnaPure (Roche Diagnostics, The Netherlands) using the total nucleic acid isolation kit.

PBMC isolation

PBMCs were isolated from EDTA blood samples. Tubes were centrifuged at 200*g* for 15 min to separate cellular parts. The plasma-containing fraction was collected, centrifuged at 1200*g* for 15 min, and the plasma was aliquoted and stored at −20°C. The cellular fraction was reconstituted with phosphate-buffered saline and subjected to Ficoll density gradient centrifugation (500*g*, 30 min). PBMCs were washed and frozen in 90% fetal bovine serum (FBS) and 10% DMSO (Sigma Life Science) at −135°C. Upon use, PBMCs were thawed in Iscove's modified Dulbecco's media (Lonza, Belgium) supplemented with 10% FBS, penicillin (100 IU/ml), streptomycin (100 μg/ml) (Lonza, Belgium), and 2 mM L-glutamine (Lonza, Belgium) (I10F medium). PBMCs were treated with Benzonase (50 U/ml; Merck) for 30 min at 37°C before use in stimulation assays.

Epitope MP design and preparation

SARS-CoV-2 virus-specific CD4 and CD8 peptides were synthesized as crude material (A&A, San Diego, CA), resuspended in DMSO, pooled, and sequentially lyophilized as previously reported (*25*). SARS-CoV-2 epitopes were predicted using the protein sequences derived from the SARS-CoV-2 reference sequence (GenBank: MN908947) and immune epitope database (IEDB) analysis-resource as previously described (*11*, *26*). Specifically, CD4 SARS-CoV-2 epitope prediction was carried out using a previously described approach in TepiTool resource in IEDB (*27*, *28*), similarly to what was previously described (*11*), but removing the resulting spike glycoprotein epitopes from this prediction [CD4-R(remainder) MP, n = 246]. To investigate in depth spike-specific $CD4^+$ T cells, overlapping 15-mer by 10 amino acids has been synthesized and pooled separately [CD-4 S(spike) MP, n = 221]. CD8 SARS-CoV-2 epitope prediction was performed as previously reported, using the NetMHCpan4.0 algorithm for the top 12 more frequent HLA alleles in the population (HLA-A*01:01, HLA-A*02:01, HLA-A*03:01, HLA-A*11:01, HLA-A*23:01, HLA-A*24:02, HLA-B*07:02, HLA-B*08:01, HLA-B*35:01, HLA-B*40:01, HLA-B*44:02, and HLA-B*44:03) and selecting the top 1 percentile predicted epitopes per HLA allele (*11*). The 628 predicted CD8 epitopes were split in two CD8 MPs containing 314 peptides each.

SARS-CoV-2 RBD ELISA

Serum or plasma samples were analyzed for the presence of SARS-CoV-2–specific antibody responses using a validated in-house SARS-CoV-2 RBD IgG ELISA as previously described (*29*). Briefly, ELISA plates were coated with recombinant SARS-CoV-2 RBD protein. After blocking, samples were added and incubated for 1 hour, after which the plates were washed and a secondary horseradish peroxidase–labeled rabbit anti-human IgG (Dako) was added. After a 1-hour

incubation, the plates were washed, the signal was developed using trimethylboron, and the OD_{450} (optical density at 450 nm) was measured for each well. Endpoint titers were determined as the highest dilution with an OD_{450} above the cutoff, which is based on the negative control. All samples reported here were interrogated for the presence of antibodies on the same plate.

Ex vivo stimulations

PBMCs were plated in 96-well U bottom plates at 1×10^6 PBMCs per well in RPMI 1640 (Lonza, Belgium) supplemented with 10% human serum, penicillin (100 IU/ml), streptomycin (100 μg/ml) (Lonza, Belgium), and 2 mM L-glutamine (Lonza, Belgium) (R10H medium) and subsequently stimulated with the described CD4 and CD8 SARS-CoV-2 MPs at 1 μg/ml. A stimulation with an equimolar amount of DMSO was performed as negative control, and PHA (1 μg/ml; Roche) and stimulation with a combined CD4 and CD8 CMV MPs (1 μg/ml) were included as positive controls. Twenty hours after, stimulation cells were stained for detection of activation-induced markers and subjected to flow cytometry. Supernatants were harvested for multiplex detection of cytokines.

Flow cytometry

Activation-induced markers were quantified via flow cytometry (FACSLyric, BD Biosciences). A surface staining on PBMC was performed with anti-$CD3^{PerCP}$ (clone SK7, BD), anti-$CD4^{V450}$ (clone L200, BD), anti-$CD8^{FITC}$ (clone DK25, Dako), anti-$CD45RA^{PE\text{-}Cy7}$ (clone L48, BD), anti-$CCR7^{APC}$ (clone 150503, R&D Systems), anti-$CD69^{APC\text{-}H7}$ (clone FN50, BD), and anti-$CD137^{PE}$ (clone 4B4-1, Miltenyi). T cell subsets were identified via the following gating strategy: LIVE $CD3^+$ T cells were selected and divided in $CD3^+CD4^+$ and $CD3^+CD8^+$. Within the CD4 and CD8 subsets, memory subsets were gated as $CD45RA^+CCR7^+$ (naive, T_N), $CD45RA^-$, $CCR7^+$ (central memory, T_{CM}), $CD45RA^-CCR7^-$ (effector memory, T_{EM}), or $CD45RA^+CCR7^-$ (terminally differentiated effectors, T_{EMRA}). T cells specifically activated by SARS-CoV-2 were identified by up-regulation of CD69 and CD137. An average of 500,000 cells was always acquired, and the gating strategy is schematically represented in fig. S1 (A to J). In analysis, PBMC stimulated with MP_CD8_A and MP_CD8_B were concatenated and analyzed as a single file for SARS-CoV-2–specific responses to MP_CD8.

Multiplex detection of cytokines

Cytokines in cell culture supernatants from ex vivo stimulations were quantified using a human T_H cytokine panel (13-plex) kit (LEGENDplex, BioLegend). Briefly, cell culture supernatants were mixed with beads coated with capture antibodies specific for IL-5, IL-13, IL-2, IL-6, IL-9, IL-10, IFN-γ, TNF-α, IL-17A, IL-17F, IL-4, IL-21, and IL-22 and incubated for 2 hours. Beads were washed and incubated with biotin-labeled detection antibodies for 1 hour, followed by a final incubation with $streptavidin^{PE}$. Beads were analyzed by flow cytometry. Analysis was performed using the LEGENDplex analysis software v8.0, which distinguishes between the 13 different analytes on the basis of bead size and internal dye. Quantity of each respective cytokine is calculated on the basis of intensity of the $streptavidin^{PE}$ signal and a freshly prepared standard curve.

Statistical analysis

For comparison of $CD3^+$ T cell percentages, CD4:CD8 ratios, $CD69^+CD137^+$-stimulated T cells, and cytokine levels between HC and patients with COVID-19, all log-transformed data were tested for normal distribution. If distributed normally, groups were compared via an unpaired *t* test. If not distributed normally, groups were compared via a Mann-Whitney test. Comparisons between different stimulations (DMSO versus MP) were performed by paired *t* test (normal distribution) or Wilcoxon rank test (no normal distribution). Two-tailed *P* values are reported throughout the manuscript. One-way ANOVA repeated measures were used to test for increasing or decreasing trends over sequential time points (0, 7, and 14 days after inclusion).

SUPPLEMENTARY MATERIALS

immunology.sciencemag.org/cgi/content/full/5/48/eabd2071/DC1

Fig. S1. Flow cytometry gating strategy.

Fig. S2. SARS-CoV-2–specific cytokine production in COVID-19 ARDS patients.

Fig. S3. Correlations between kinetics of viral loads, virus-specific antibodies, and virus-specific T cell responses.

Table S1. Raw data (in Excel spreadsheet).

View/request a protocol for this paper from *Bio-protocol*.

REFERENCES AND NOTES

1. J. F.-W. Chan, S. Yuan, K.-H. Kok, K. K.-W. To, H. Chu, J. Yang, F. Xing, J. Liu, C. C.-Y. Yip, R. W.-S. Poon, H.-W. Tsoi, S. K.-F. Lo, K.-H. Chan, V. K.-M. Poon, W.-M. Chan, J. D. Ip, J.-P. Cai, V. C.-C. Cheng, P. H. Chen, C. K.-M. Hui, K.-Y. Yuen, A familial cluster of pneumonia associated with the 2019 novel coronavirus indicating person-to-person transmission: A study of a family cluster. *Lancet* **395**, 514–523 (2020).
2. C. Huang, Y. Wang, X. Li, L. Ren, J. Zhao, Y. Hu, L. Zhang, G. Fan, J. Xu, X. Gu, Z. Cheng, T. Yu, J. Xia, Y. Wei, W. Wu, X. Xie, W. Yin, H. Li, M. Liu, Y. Xiao, H. Gao, L. Guo, J. Xie, G. Wang, R. Jiang, Z. Gao, Q. Jin, J. Wang, B. Cao, Clinical features of patients infected with 2019 novel coronavirus in Wuhan, China. *Lancet* **395**, 497–506 (2020).
3. G. Chen, D. Wu, W. Guo, Y. Cao, D. Huang, H. Wang, T. Wang, X. Zhang, H. Chen, H. Yu, X. Zhang, M. Zhang, S. Wu, J. Song, T. Chen, M. Han, S. Li, X. Luo, J. Zhao, Q. Ning, Clinical and immunologic features in severe and moderate coronavirus disease 2019. *J. Clin. Invest.* **130**, 2620–2629 (2020).
4. P. Mehta, D. F. McAuley, M. Brown, E. Sanchez, R. S. Tattersall, J. J. Manson; HLH Across Speciality Collaboration, UK, COVID-19: Consider cytokine storm syndromes and immunosuppression. *Lancet* **395**, 1033–1034 (2020).
5. Z. Xu, L. Shi, Y. Wang, J. Zhang, L. Huang, C. Zhang, S. Liu, P. Zhao, H. Liu, L. Zhu, Y. Tai, C. Bai, T. Gao, J. Song, P. Xia, J. Dong, J. Zhao, F.-S. Wang, Pathological findings of COVID-19 associated with acute respiratory distress syndrome. *Lancet Respir. Med.* **8**, 420–422 (2020).
6. I. Thevarajan, T. H. O. Nguyen, M. Koutsakos, J. Druce, L. Caly, C. E. van de Sandt, X. Jia, S. Nicholson, M. Catton, B. Cowie, S. Y. C. Tong, S. R. Lewin, K. Kedzierska, Breadth of concomitant immune responses prior to patient recovery: A case report of non-severe COVID-19. *Nat. Med.* **26**, 453–455 (2020).
7. L. Ni, F. Ye, M.-L. Cheng, Y. Feng, Y.-Q. Deng, H. Zhao, P. Wei, J. Ge, M. Gou, X. Li, L. Sun, T. Cao, P. Wang, C. Zhou, R. Zhang, P. Liang, H. Guo, X. Wang, C.-F. Qin, F. Chen, C. Dong, Detection of SARS-CoV-2-specific humoral and cellular immunity in COVID-19 convalescent individuals. *Immunity* **52**, 971–977.e3 (2020).
8. A. Grifoni, D. Weiskopf, S. I. Ramirez, J. Mateus, J. M. Dan, C. R. Moderbacher, S. A. Rawlings, A. Sutherland, L. Premkumar, R. S. Jadi, D. Marrama, A. M. de Silva, A. Frazier, A. F. Carlin, J. A. Greenbaum, B. Peters, F. Krammer, D. M. Smith, S. Crotty, A. Sette, Targets of T cell responses to SARS-CoV-2 coronavirus in humans with COVID-19 disease and unexposed individuals. *Cell* **181**, 1489–1501.e15 (2020).
9. C. K.-f. Li, H. Wu, H. Yan, S. Ma, L. Wang, M. Zhang, X. Tang, N. J. Temperton, R. A. Weiss, J. M. Brenchley, D. C. Douek, J. Mongkolsapaya, B.-H. Tran, C.-I. S. Lin, G. R. Screaton, J.-l. Hou, A. J. McMichael, X.-N. Xu, T cell responses to whole SARS coronavirus in humans. *J. Immunol.* **181**, 5490–5500 (2008).
10. J. Zhao, A. N. Alshukairi, S. A. Baharoon, W. A. Ahmed, A. A. Bokhari, A. M. Nehdi, L. A. Layqah, M. G. Alghamdi, M. M. Al Gethamy, A. M. Dada, I. Khalid, M. Boujelal, S. M. Al Johani, L. Vogel, K. Subbarao, A. Mangalam, C. Wu, P. T. Eyck, S. Perlman, J. Zhao, Recovery from the Middle East respiratory syndrome is associated with antibody and T-cell responses. *Sci Immunol* **2**, eaan5393 (2017).
11. A. Grifoni, J. Sidney, Y. Zhang, R. H. Scheuermann, B. Peters, A. Sette, A sequence homology and bioinformatic approach can predict candidate targets for immune responses to SARS-CoV-2. *Cell Host Microbe* **27**, 671–680.e2 (2020).
12. S. M. Kissler, C. Tedijanto, E. Goldstein, Y. H. Grad, M. Lipsitch, Projecting the transmission dynamics of SARS-CoV-2 through the postpandemic period. *Science* **368**, 860–868 (2020).

13. Y. D. Mahnke, T. M. Brodie, F. Sallusto, M. Roederer, E. Lugli, The who's who of T-cell differentiation: Human memory T-cell subsets. *Eur. J. Immunol.* **43**, 2797–2809 (2013).
14. F. Sallusto, D. Lenig, R. Förster, M. Lipp, A. Lanzavecchia, Two subsets of memory T lymphocytes with distinct homing potentials and effector functions. *Nature* **401**, 708–712 (1999).
15. F. Sallusto, J. Geginat, A. Lanzavecchia, Central memory and effector memory T cell subsets: Function, generation, and maintenance. *Annu. Rev. Immunol.* **22**, 745–763 (2004).
16. Z. Wang, A. Zhang, Y. Wan, X. Liu, C. Qiu, X. Xi, Y. Ren, J. Wang, Y. Dong, M. Bao, L. Li, M. Zhou, S. Yuan, J. Sun, Z. Zhu, L. Chen, Q. Li, Z. Zhang, X. Zhang, S. Lu, P. C. Doherty, K. Kedzierska, J. Xu, Early hypercytokinemia is associated with interferon-induced transmembrane protein-3 dysfunction and predictive of fatal H7N9 infection. *Proc. Natl. Acad. Sci. U.S.A.* **111**, 769–774 (2014).
17. Y. Peng, A. J. Mentzer, G. Liu, X. Yao, Z. Yin, D. Dong, W. Dejnirattisai, T. Rostron, P. Supasa, C. Liu, C. Lopez-Camacho, J. Slon-campos, Y. Zhao, D. Stuart, G. Paeson, J. Grimes, F. Antson, O. W. Bayfield, D. E. D. P. Hawkins, D.-S. Ker, L. Turtle, K. Subramaniam, P. Thomson, P. Zhang, C. Dold, J. Ratcliff, P. Simmonds, T. de Silva, P. Sopp, D. Wellington, U. Rajapaksa, Y.-L. Chen, M. Salio, G. Napolitani, W. Paes, P. Borrow, B. Kessler, J. W. Fry, N. F. Schwabe, M. G. Semple, K. J. Baillie, S. Moore, P. J. M. Openshaw, A. Ansari, S. Dunachie, E. Barnes, J. Frater, G. Kerr, P. Goulder, T. Lockett, R. Levin; Oxford Immunology Network Covid- Response T cell Consortium, R. J. Cornall, C. Conlon, P. Klenerman, A. M. Michael, G. Screaton, J. Mongkolsapaya, J. C. Knight, G. Ogg, T. Dong, Broad and strong memory CD4$^+$ and CD8$^+$T cells induced by SARS-CoV-2 in UK convalescent COVID-19 patients. *BioRxiv* 10.1101/2020.06.05.134551v1 (2020).
18. T. Herold, V. Jurinovic, C. Arnreich, B. J. Lipworth, J. C. Hellmuth, M. von Bergwelt-Baildon, M. Klein, T. Weinberger, Elevated levels of IL-6 and CRP predict the need for mechanical ventilation in COVID-19. *J. Allergy Clin. Immunol.* 10.1016/j.jaci.2020.05.008 (2020).
19. J. Braun, L. Loyal, M. Frentsch, D. Wendisch, P. Georg, F. Kurth, S. Hippenstiel, M. Dingeldey, B. Kruse, F. Fauchere, E. Baysal, M. Mangold, L. Henze, R. Lauster, M. Mall, K. Beyer, J. Roehmel, J. Schmitz, S. Miltenyi, M. A. Mueller, M. Witzenrath, N. Suttorp, F. Kern, U. Reimer, H. Wenschuh, C. Drosten, V. M. Corman, C. Giesecke-Thiel, L.-E. Sander, A. Thiel, Presence of SARS-CoV-2 reactive T cells in COVID-19 patients and healthy donors. *MedRxiv* 10.1101/2020.04.17.20061440 (2020).
20. N. Le Bert, A. T. Tan, K. Kunasegaran, C. Y. L. Tham, M. Hafezi, A. Chia, M. Chng, M. Lin, N. Tan, M. Linster, W. N. Chia, M. I.-C. Chen, L.-F. Wang, E. E. Ooi, S. Kalimuddin, P. A. Tambyah, J. G.-H. Low, Y.-J. Tan, A. Bertoletti, Different pattern of pre-existing SARS-COV-2 specific T cell immunity in SARS-recovered and uninfected individuals. *BioRxiv* 10.1101/2020.05.26.115832 (2020).
21. B. J. Meckiff, C. Ramírez-Suástegui, V. Fajardo, S. J. Chee, A. Kusnadi, H. Simon, A. Grifoni, E. Pelosi, D. Weiskopf, A. Sette, F. Ay, G. Seumois, C. H. Ottensmeier, P. Vijayanand, Single-cell transcriptomic analysis of SARS-CoV-2 reactive CD4$^+$T cells. *BioRxiv* 10.1101/2020.06.12.148916, (2020).
22. C. J. Thieme, M. Anft, K. Paniskaki, A. Blazquez-Navarro, A. Doevelaar, F. S. Seibert, B. Hoelzer, M. J. Konik, T. Brenner, C. Tempfer, C. Watzl, S. Dolff, U. Dittmer, T. H. Westhoff, O. Witzke, U. Stervbo, T. Roch, N. Babel, The SARS-CoV-2 T-cell immunity is directed against the spike, membrane, and nucleocapsid protein and associated with COVID 19 severity. *MedRxiv* 10.1101/2020.05.13.20100636 (2020).
23. E. Gimenez, E. Albert, I. Torres, M. J. Remigia, M. J. Alcaraz, M. J. Galindo, M. L. Blasco, C. Solano, M. J. Forner, J. Redon, J. Signes-Costa, D. Navarro, SARS-CoV-2-reactive interferon-γ-producing CD8+ T cells in patients hospitalized with Coronavirus viral disease-2019. *MedRxiv* 10.1101/2020.05.18.20106245 (2020).
24. V. M. Corman, O. Landt, M. Kaiser, R. Molenkamp, A. Meijer, D. K. W. Chu, T. Bleicker, S. Brünink, J. Schneider, M. L. Schmidt, D. G. J. C. Mulders, B. L. Haagmans, B. van der Veer, S. van den Brink, L. Wijsman, G. Goderski, J.-L. Romette, J. Ellis, M. Zambon, M. Peiris, H. Goossens, C. Reusken, M. P. G. Koopmans, C. Drosten, Detection of 2019 novel coronavirus (2019-nCoV) by real-time RT-PCR. *Euro Surveill.* **25**, 2000045 (2020).
25. S. Carrasco Pro, J. Sidney, S. Paul, C. L. Arlehamn, D. Weiskopf, B. Peters, A. Sette, Automatic generation of validated specific epitope sets. *J. Immunol. Res.* **2015**, 763461 (2015).
26. S. K. Dhanda, S. Mahajan, S. Paul, Z. Yan, H. Kim, M. C. Jespersen, V. Jurtz, M. Andreatta, J. A. Greenbaum, P. Marcatili, A. Sette, M. Nielsen, B. Peters, IEDB-AR: Immune epitope database-analysis resource in 2019. *Nucleic Acids Res.* **47**, W502–W506 (2019).
27. S. Paul, C. S. L. Arlehamn, T. J. Scriba, M. B. C. Dillon, C. Oseroff, D. Hinz, D. M. McKinney, S. C. Pro, J. Sidney, B. Peters, A. Sette, Development and validation of a broad scheme for prediction of HLA class II restricted T cell epitopes. *J. Immunol. Methods* **422**, 28–34 (2015).
28. S. Paul, J. Sidney, A. Sette, B. Peters, TepiTool: A pipeline for computational prediction of T cell epitope candidates. *Curr. Protoc. Immunol.* **114**, 18.19.1–18.19.24 (2016).
29. N. M. A. Okba, M. A. Müller, W. Li, C. Wang, C. H. G. Kessel, V. M. Corman, M. M. Lamers, R. S. Sikkema, E. de Bruin, F. D. Chandler, Y. Yazdanpanah, Q. L. Hingrat, D. Descamps, N. Houhou-Fidouh, C. B. E. M. Reusken, B.-J. Bosch, C. Drosten, M. P. G. Koopmans, B. L. Haagmans, Severe acute respiratory syndrome coronavirus 2-specific antibody responses in coronavirus disease 2019 patients. *Emerg. Infect. Dis.* **26**, 1478–1488 (2020).

Acknowledgments: We thank all health care workers and laboratory personnel who contributed to treatment and diagnosis of these and other patients with COVID-19. Specifically, we thank J. van Kampen, C. Geurts van Kessel, A. van der Eijk, and M. Lammers for contributions to these studies. **Funding:** This work has received funding from the European Union's Horizon 2020 research and innovation program under grant agreements no. 874735 (VEO) (to M.P.G.K., E.C.M.v.G, and M.P.R.). This work was also funded by the NIH contract no. 75N9301900065 (to A.S. and D.W.). **Author contributions:** D.W., A.G., R.L.d.S., A.S., and R.D.d.V. conceived and planned the experiments. D.W., K.S.S., M.P.R., N.M.A.O., R.M., and E.C.M.v.G. contributed to sample preparation. D.W., K.S.S., M.P.R., A.G., N.M.A.O., H.E., J.P.C.v.s.A., R.M., and R.D.d.V. carried out the experiments. D.W., K.S.S., A.G., M.P.G.K., B.L.H., R.L.d.S., A.S., and R.D.d.V. contributed to the interpretation of the results. R.D.d.V. took the lead in writing the manuscript, and D.W., K.S.S., and R.L.d.S. contributed significantly. All authors provided critical feedback and helped shape the research, analysis, and manuscript. **Competing interests:** A.S. is listed as inventor on a provisional patent application covering findings reported in this manuscript. A.S. is a consultant for Gritstone, Flow Pharma Inc. and Avalia. All other authors declare that they have no competing interests. **Data and materials availability:** Epitope MPs used in this paper will be made available to the scientific community upon request and execution of a material transfer agreement. Please direct requests to D.W. at daniela@lji.org. All data needed to evaluate the conclusions in the paper are present in the paper or the Supplementary Materials.

Submitted 8 June 2020
Accepted 24 June 2020
Published First Release 26 June 2020
Final published 13 July 2020

10.1126/sciimmunol.abd2071

Citation: D. Weiskopf, K. S. Schmitz, M. P. Raadsen, A. Grifoni, N. M. A. Okba, H. Endeman, J. P. C. van den Akker, R. Molenkamp, M. P. G. Koopmans, E. C. M. van Gorp, B. L. Haagmans, R. L. de Swart, A. Sette, R. D. de Vries, Phenotype and kinetics of SARS-CoV-2–specific T cells in COVID-19 patients with acute respiratory distress syndrome. *Sci. Immunol.* **5**, eabd2071 (2020).

Science Immunology

Phenotype and kinetics of SARS-CoV-2–specific T cells in COVID-19 patients with acute respiratory distress syndrome

Daniela Weiskopf, Katharina S. Schmitz, Matthijs P. Raadsen, Alba Grifoni, Nisreen M. A. Okba, Henrik Endeman, Johannes P. C. van den Akker, Richard Molenkamp, Marion P. G. Koopmans, Eric C. M. van Gorp, Bart L. Haagmans, Rik L. de Swart, Alessandro Sette and Rory D. de Vries

Sci. Immunol. **5**, eabd2071.
First published 26 June 2020
DOI: 10.1126/sciimmunol.abd2071

Tracking antiviral T cells in COVID-19

In patients infected with SARS-CoV-2, T lymphocytes stimulated by fragments of viral proteins contribute to immunity but may also promote the development of "cytokine storm." Weiskopf *et al.* studied the emergence of antiviral T cells in the blood of 10 patients with severe COVID-19 requiring ventilator treatment by stimulating blood lymphocytes with pools of peptides based on viral protein sequences. Peptide-reactive $CD4^+$ and $CD8^+$ T cells were already detectable at ICU admission and generally increased over time. Two of the 10 healthy controls responded weakly to the peptides, suggesting that some T cells induced by common cold coronaviruses can cross-react with SARS-CoV-2 antigens. These foundational studies set the stage for future experiments to tease apart the dynamics of T cell clones specific for different viral antigens.

Science Immunology (ISSN 2470-9468) is published by the American Association for the Advancement of Science, 1200 New York Avenue NW, Washington, DC 20005. The title *Science Immunology* is a registered trademark of AAAS.